ISSN 1063-7834, Physics of the Solid State, 2022. © Pleiades Publishing, Ltd., 2022.
Russian Text © The Author(s), 2022, published in Fizika Tverdogo Tela, 2022, Vol. 64, No. 9, pp. 1223–1227.

Josephson Tunnel Junctions with an Integral Superconductor–Insulator–Normal Metal Shunt

M. S. Shevchenko[a, b, *], L. V. Filippenko[a], O. S. Kiselev[a, c], and V. P. Koshelets[a, c]

[a] *Kotel'nikov Institute of Radio Engineering and Electronics, Russian Academy of Sciences, Moscow, 125009 Russia*
[b] *Moscow Institute of Physics and Technology, Dolgoprudny, Moscow oblast, 141701 Russia*
[c] *Institute of Physics of Microstructures, Russian Academy of Sciences, GSP-105, Moscow, 603950 Russia*
**e-mail: shevchenko@hitech.cplire.ru*

Received April 29, 2022; revised April 29, 2022; accepted May 12, 2022

Abstract—This study is devoted to the investigation of tunneling superconductor–insulator–superconductor (SIS) Josephson junctions with a new type of shunt based on an additional superconductor–insulator–normal metal (SIN) junction placed around the SIS junction. In the course of study, the parameters of such shunted junctions are numerically calculated and their current–voltage characteristics (IVC) are simulated. The designed structures are assembled in real samples and their parameters are studied; the IVC of junctions with different degrees of shunting are measured, and the behavior of these junctions under the influence of high-frequency signals in the subterahertz range is studied.

Keywords: superconducting devices, superconductor–insulator–superconductor tunnel junction, Josephson effect, Josephson junction shunting

DOI: 10.1134/S1063783422060075

1. INTRODUCTION

Shunted Josephson junctions are needed to create generators and receivers of terahertz and subterahertz radiation, superconducting quantum interferometers (SQUIDs), and single-quantum digital devices. Shunting provides a hysteresis-free current–voltage characteristic (IVC) while maintaining a sufficiently high characteristic voltage (and, accordingly, characteristic frequency) [1]. Normally, thin-film resistors are used as a shunt [2, 3], but this method has disadvantages (large size of the structure and high parasitic inductance, which reduce the operating frequency of devices) [4]. A new type of shunting was proposed to eliminate these drawbacks, which consists in the creation of superconductor–insulator–superconductor (SIS) tunnel junctions with integral shunting by means of a superconductor–insulator–normal metal (SIN) junction arranged around the main junction. The junctions are manufactured with it in the same technological process (Fig. 1). The inner radius of the SIN junction is determined by the radius of the SIS junction, while the outer radius is selected taking into account the required resistance. A more detailed description of the manufacturing technology and the first study results are given in [5].

The new method of shunting by means of a SIN junction can substantially reduce the overall size of the topology and, consequently, reduce the parasitic inductance of the shunt, which has a positive effect on its operation in the high-frequency range. There are other ways of internal shunting, which also allow one to reduce the size of the structure. There is a method of shunting by creating junctions with a very high current density [2], but with this method requires production of small size junctions (junction areas less than 0.1 μm^2) with a very thin insulator layer (about several atomic layers), and such a process is difficult to control. Another way is to fabricate a Josephson junction with a layer of a conducting material, for example, $Nb_{1-y}Ti_yN/Ta_xN/Nb_{1-y}Ti_yN$ [6]. The poor reproducibility of the required parameters is a disadvantage of this method of shunting. The conducted studies [7] indicate that critical currents I_c and normal resistances R_n vary greatly even for samples fabricated on the same substrate because of violation of stoichiometry.

Thus, the proposed method of integral SIN shunting has a number of advantages in comparison with its analogues. This study is devoted to studying the characteristics of such junctions.

2. SIMULATION

To determine the geometric parameters of junctions with a high characteristic voltage of $V_c = I_cR$ (I_c is the critical current of the Josephson junction, R is the total resistance of the shunt and the junction at voltages below the energy gap) and non-hysteretic IVC (in this case, McCumber's parameter β_c =

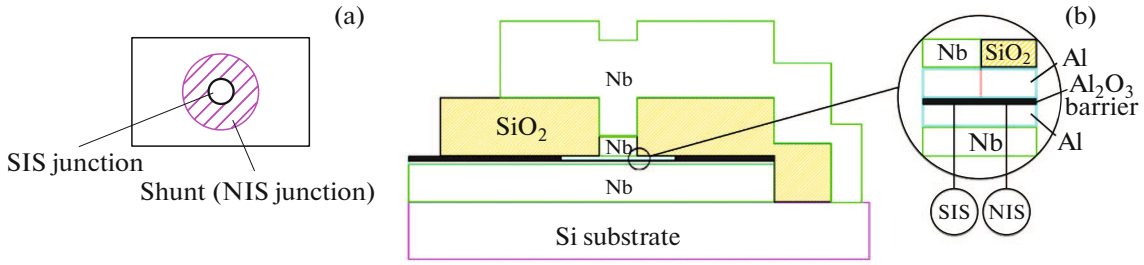

Fig. 1. (a) Diagram for integrated shunting with use a SIN junction; (b) section of the circuit.

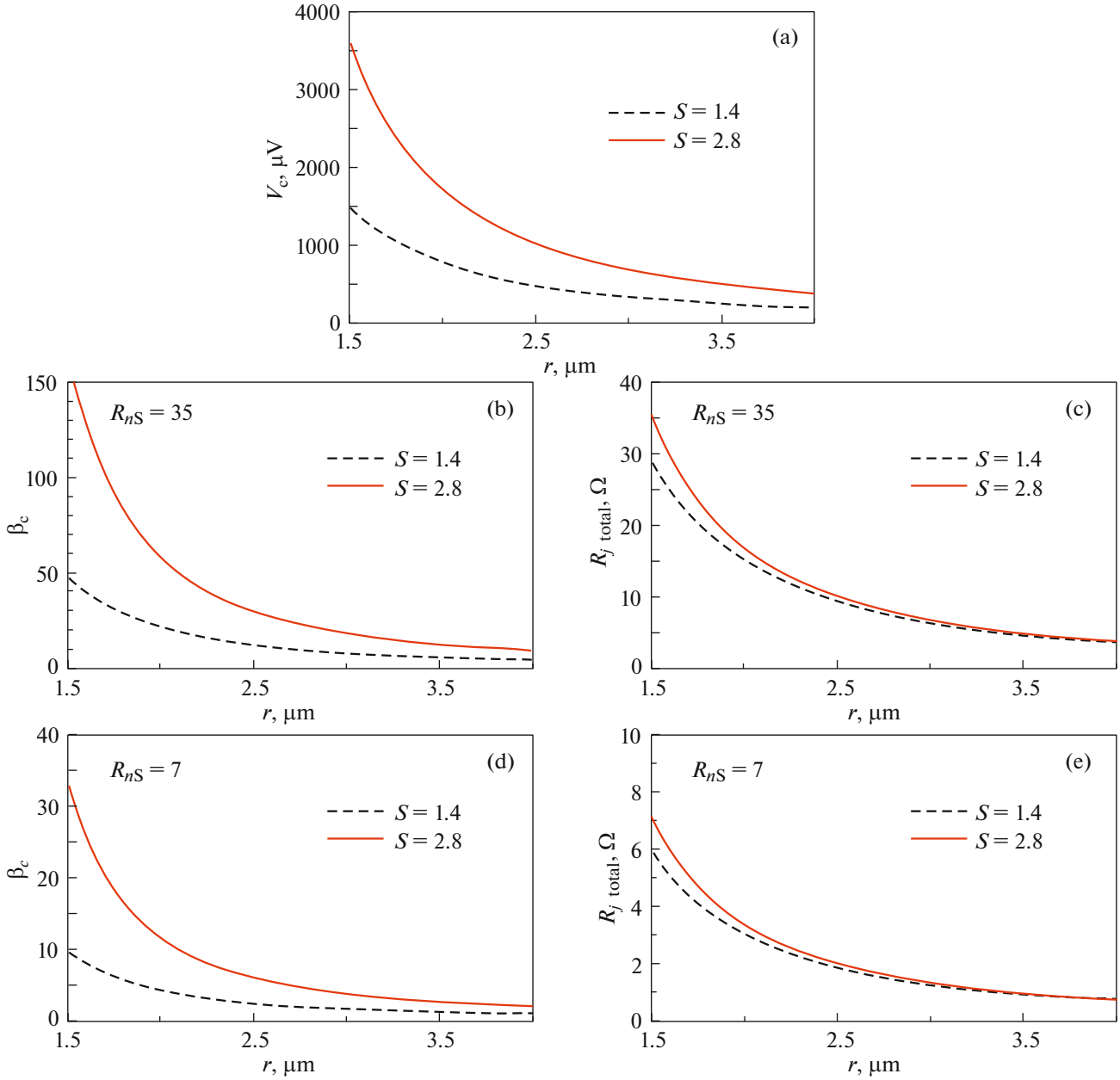

Fig. 2. Calculation of the parameters of the junction with SIN shunting as functions of the outer radius of the shunt and for SIN junction areas of 1.4 and 2.8 μm^2: (a) characteristic voltage V_c, (b) hysteresis parameter β_c, and (c) total voltage $R_{j\,total}$ of the shunt and junction below the energy gap for specific tunneling resistance $R_{nS} = 35\ \Omega\,\mu m^2$; (d) β_c and (e) total voltage R_{jtotal} of the shunt and junction below the energy gap for specific tunneling resistance $R_{nS} = 7\ \Omega\,\mu m^2$.

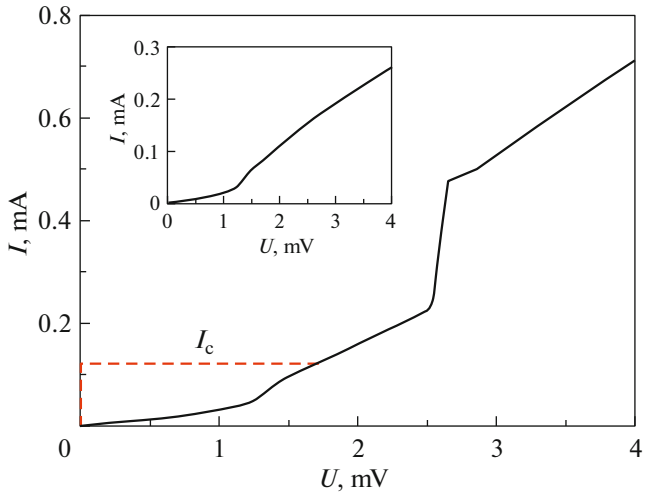

Fig. 3. Numerical calculation of the quasiparticle branch of the current–voltage characteristic of the Nb–Al/AlO_x–Nb junction shunted by the SIN junction for $T = 4.2$ K. The inset shows the IVC of the Al–AlO_x–Nb SIN junction used for shunting. The radius of the SIN junction is $r_1 = 0.95$ μm; the outer radius of the shunt is $r_2 = 2$ μm; the specific tunneling resistance is $R_{nS} = 30\ \Omega\ \mu m^2$; the calculated parameters of junctions with the same sizes and R_{nS} are as follows: $V_c = 1300$ μV and $\beta_c = 30$. The dotted line shows the calculated value of the critical current in the straight branch.

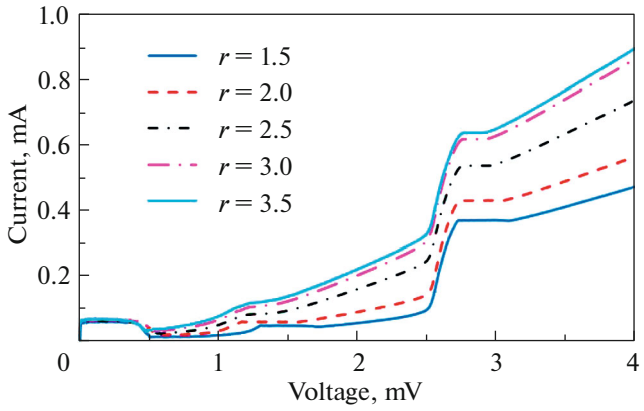

Fig. 4. Experimental IVCs of junctions with integrated SIN shunting. The measurements were performed in the mode of set voltage. The SIN junction area is $S = 1.4\ \mu m^2$. The outer radius of the shunt ranges from 1.5 to 3.5 μm.

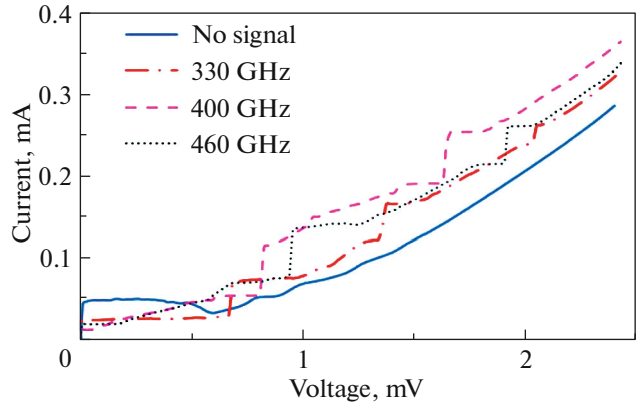

Fig. 5. Current–voltage characteristics of junctions with integral SIN shunting without signal stimulus and under the influence of signals with frequencies of 330, 400, and 460 GHz. Shapiro steps are observed at voltages of $V_n = n\hbar\omega/2e$.

$(2\pi/\Phi_0)I_cR^2C \lesssim 1$ [1, 8], where Φ_0 is the quantum of the magnetic flux, and C is the junction capacitance), numerical calculations were performed (Fig. 2). The radius of the SIN shunt varied from 1.5 to 4 μm.

As can be seen from Fig. 2, shows that in order to achieve a higher characteristic voltage at lower β_c, it is required to fabricate junctions with a high current density (low specific tunneling resistance R_{nS}).

Within numerical simulation, the current–voltage characteristic (Fig. 3) of the junction with an integrated SIN shunt was also calculated using the expression for the analytical IVCs of the SIN junction [9]. The developed numerical models make it possible to determine what will be the parameters of the junctions with a given current density and geometric dimensions of the SIS junction and the shunt. In addition, the parameters necessary to obtain junctions with the necessary properties can also be determined.

3. EXPERIMENTAL

Designed junction samples were fabricated and studied. Figure 4 shows the experimental IVCs of samples with integrated SIN shunting for various external radii of the shunt. As can be seen from Fig. 4, the proposed design of the shunt is really functioning.

The characteristics of shunted structures exposed to an alternating current signal were also studied. A distributed Josephson junction, so called flux-flow oscillator (FFO [10, 11] operating in the range of 300–700 GHz was used as a generator; it was arranged on the same substrate as the shunted structure did. Figure 5 shows the IVCs of the shunted junction without exposure to the current signal and under the influence of signals with frequencies of 330, 400, and 460 GHz (at voltages $V_n = n\hbar\omega/2e$, the corresponding Shapiro steps due to synchronization of the Josephson generation by an external signal are observed), from which we can conclude that the new type of shunting keeps functioning at high frequencies as well.

Figure 6a shows the IVCs of the junction with an integral SIN shunt at different strengths of a signal with a frequency of 410 GHz. The current–voltage characteristics were measured to obtain the depen-

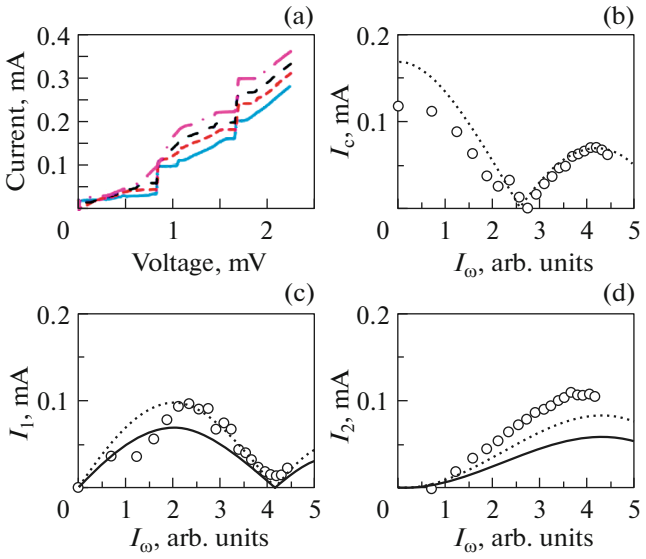

Fig. 6. (a) Current–voltage characteristics of a junction with SIN shunting under the influence of FFO signals of different powers at a frequency of 410 GHz; (b) the double amplitude of critical current I_c, the amplitudes of the (c) first (I_1) and (d) second (I_2) Shapiro steps as functions of the amplitude of high-frequency signal current I_ω in relative units. The dots show experimental data; the solid lines show dependences for the resistive model consistent with the experiment at $I_\omega = 0$; the same dependences consistent with the experiment at $I_\omega = 4$ are shown by dotted lines.

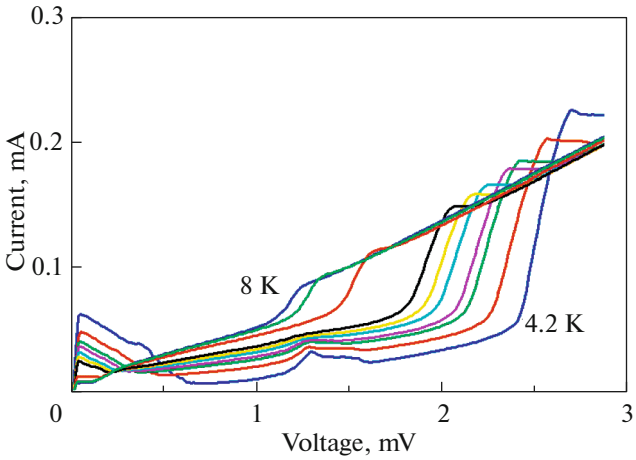

Fig. 7. Current–voltage characteristics of the junction with SIN shunting at various temperatures in the range from 4.2 to 8 K. The area of the junction is $S = 1.4$ μm^2; the outer radius of the SIN junction is $r = 1.5$ μm.

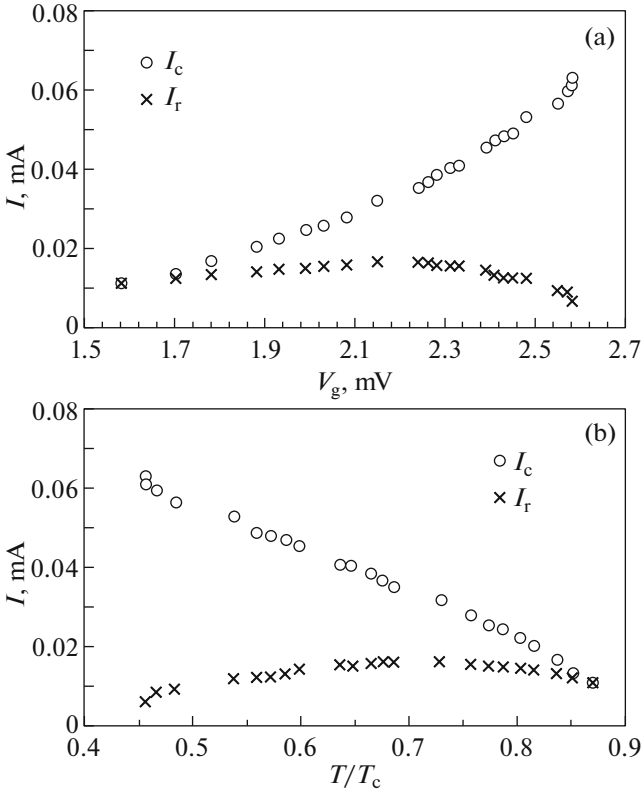

Fig. 8. (a) Dependences of critical current I_c and return current I_r on gap voltage V_g, and (b) the temperature dependenced of critical current I_c and return current I_r (estimated from V_g). $T_c = 9.2$ K.

dences for the double amplitude of the critical current and the amplitudes of the 1st and 2nd Shapiro stages, as well as to estimate the V_c value from high-frequency measurements. The amplitude of the step with number n under provision that frequency ω of the external periodic signal is less than or equal to characteristic transition frequency $\omega_c = 2eV_c/\hbar$ is expressed by formula $I_n^{\pm} = I_c J_n(I_\omega/I_c)$ [1], where J_n is the Bessel function of the first kind of the nth order, and I_ω is the amplitude of the external signal.

The amplitudes of the first steps were measured for different frequencies as functions of the generator power, which varied due to a change in the FFO current at a constant voltage (frequency) [10]. Figures 6b–6d show the dependences of the doubled critical current and the amplitude of the first two current steps on amplitude I_ω of the current signal at a frequency of 410 GHz, which is proportional, in the first approximation, to the root of the FFO superconducting current at a voltage of 1 mV [11].

Solid lines and dotted lines show the dependences constructed on the basis of the resistive model of transitions with low damping [1, 12], i.e., the Bessel functions of the corresponding order. These dependences make it possible to estimate characteristic voltage V_c^{RF} of the shunted junction at high frequency [1]; the good agreement between the oscillations and the unmodified Bessel function at a frequency of 410 GHz suggests that the V_c^{RF} value of is about 0.8 mV.

The I–V characteristics of shunted junctions were measured at various temperatures in the range from 4.2 to 8 K (Fig. 7). Based on the results of these measurements, the dependences of critical current I_c and return current I_r as functions of the value of gap voltage V_g were plotted (Fig. 8a). The temperature was estimated from the V_g value [13, 14]; the results are given in Fig. 8b.

As can be seen from Fig. 8, the I_r/I_c ratio tends to 1 with a decrease in the critical current and, accordingly, parameter $\beta_c = (2\pi/\Phi_0)I_cR^2C$, as predicted in [1]; that is, the IVC of the transition becomes non-hysteretic. The results given in Fig. 8b correspond to the results of calculations performed in [13] within the microscopic superconductivity theory taking into account the effect of the proximity of a bulk superconductor and a thin film of normal metal for superconductor–normal metal–insulator–normal metal–superconductor (SNINS) structures.

4. CONCLUSIONS

The novel design of junctions with integral shunting by means of a SIN junction is developed. The numerical simulation is performed, and the following parameters of such junctions are calculated: the total resistance of the shunt and the SIS junction, the characteristic voltage, and the McCumber hysteresis parameter. Junction samples are assembled, and their IVCs and their behavior under the influence of a high-frequency signal are studied. As can be concluded from the study results, the proposed method of shunting is really effective, including the operation at high frequencies. The characteristic voltage from high-frequency measurements can be estimated by a value of 0.8 mV from below (frequency 400 GHz). Temperature dependences are also measured, which show how the critical current of the junction and, accordingly, the characteristic voltage behave as functions of the energy gap (temperature).

FUNDING

This study was supported by the Russian Science Foundation (project no. 20-42-04415). Tunnel junctions were made within the framework of State assignment in the Kotel'nikov Institute of Radio Engineering, Russian Academy of Sciences. To prepare samples, the equipment of enterprise USU #352529 Cryointegral was used, the development of which was supported by a grant from the Ministry of National Defense of Russian Federation (agreement no. 075-15-2021-667).

CONFLICT OF INTEREST

The authors declare that they have no conflicts of interest.

REFERENCES

1. K. K. Likharev, *Dynamics of Josephson Junctions and Circuits* (Nauka, Moscow, 1985; CRC, Boca Raton, FL, 1986).
2. S. K. Tolpygo, V. Bolkhovsky, S. Zarr, T. J. Weir, A. Wynn, A. L. Day, L. M. Johnson, and M. A. Goukeryu, IEEE Trans. Appl. Supercond. **27** (4), 1 (2017).
3. Tiantian Liang, Guofeng Zhang, Wentao Wu, Yongliang Wang, Lu Zhang, Hua Jin, Xue Zhang, Liliang Ying, and Bo Gao, IEEE Trans. Appl. Supercond. **30** (7), 1 (2020).
4. C. B. Whan and C. J. Lobb, J. Appl. Phys. **77**, 382 (1995).
5. M. S. Shevchenko, A. A. Atepalikhin, F. V. Khan, L. V. Filippenko, A. M. Chekushkin, and V. P. Koshelets, IEEE Trans. Appl. Supercond. **32** (4), 1 (2021).
6. T. van Duzer, L. Zheng, X. Meng, C. Loyo, S. R. Whiteley, L. Yu, N. Newman, J. M. Rowel, and N. Yoshikawa, Phys. C (Amsterdam, Neth.) **372**, 1 (2002).
7. L. Yu, R. Gandikota, R. K. Singh, Lin Gu, D. J. Smith, X. Meng, and X. Zeng, Supercond. Sci. Technol. **19**, 719 (2006).
8. D. E. McCumber, J. Appl. Phys. **39**, 3113 (1968).
9. D. Chouvaev, *Normal Metal Hot-Electron Microbolometer with Superconducting Andreev Mirrors* (Chalmers Univ. Technol., 2001).
10. P. N. Dmitriev, L. V. Filippenko, and V. P. Koshelets, *Josephson Junctions* (Jenny Stanford, 2017), p. 185.
11. D. R. Gulevich, V. P. Koshelets, and F. V. Kusmartsev, Phys. Rev. B **96**, 024515 (2017).
12. K. K. Likharev. Rev. Mod. Phys. **51**, 101 (1979).
13. A. A. Golubov and M. Yu. Kupriyanov, Sov. Phys. JETP **69**, 805 (1989).
14. A. A. Golubov, E. P. Houwman, J. G. Gijsbertsen, V. M. Krasnov, J. Flokstra, H. Rogalla, and M. Y. Kupriyanov, Phys. Rev. B **51**, 1073 (1995).

Translated by O. Kadkin